CSIRO PUBLISHING

Functional Plant Biology, 2021, **48**, 1062–1073
https://doi.org/10.1071/FP20225

Microgravity modelling by two-axial clinorotation leads to scattered organisation of cytoskeleton in *Arabidopsis* seedlings

Gregory Pozhvanov [A,B,C,D], *Elena Sharova* [A] *and Sergei Medvedev* [A,D]

[A]Department of Plant Physiology and Biochemistry, Faculty of Biology, St. Petersburg State University, Universitetskaya emb. 7–9, St. Petersburg 199034, Russian Federation.
[B]Laboratory of Analytical Phytochemistry, Komarov Botanical Institute, Russian Academy of Sciences, Professora Popova st. 2, St. Petersburg 197376, Russian Federation.
[C]Herzen State Pedagogical University of Russia, 48 Moika Emb., St. Petersburg 191186, Russian Federation.
[D]Corresponding authors. Emails: pozhvanov@binran.ru; s.medvedev@spbu.ru

Abstract. Proper plant development in a closed ecosystem under weightlessness will be crucial for the success of future space missions. To supplement spaceflight experiments, such conditions of microgravity are modelled on Earth using a two-axial (2A) clinorotation, and in several fundamental studies resulted in the data on proteome and metabolome adjustments, embryo development, cell cycle regulation, etc. Nevertheless, our understanding of the cytoskeleton responses to the microgravity is still limited. In the present work, we study the adjustment of actin microfilaments (MFs) and microtubules (MTs) in *Arabidopsis thaliana* (L.) Heynh. seedlings under 2A clinorotation. Modelled microgravity resulted in not only the alteration of seedlings phenotype, but also a transient increase of the hydrogen peroxide level and in the cytoskeleton adjustment. Using *GFP-fABD2* and *Lifeact-Venus* transgenic lines, we demonstrate that MFs became 'scattered' in elongating root and hypocotyl cells under 2A clinorotation. In addition, in *GFP-MAP4* and *GFP-TUA6* lines the tubulin cytoskeleton had higher fractions of transverse MTs under 2A clinorotation. Remarkably, the first static gravistimulation of continuously clinorotated seedlings reverted MF organisation to a longitudinal one in roots within 30 min. Our data suggest that the 'scattered' organisation of MFs in microgravity can serve as a good basis for the rapid cytoskeleton conversion to a 'longitudinal' structure under the gravity force.

Keywords: 3D clinostat, microfilaments, microtubules, seedling development, hydrogen peroxide, weightlessness, microgravity.

Received 30 July 2020, accepted 23 June 2021, published online 10 August 2021

Introduction

For long-term space exploration to succeed, self-sustaining life support systems adapted to conditions of microgravity must be developed. Plants are a necessary part of any closed ecosystem. For millions of years, they have been evolving in the gravity field of Earth. Plants rely on the gravity vector to establish and maintain the polarity of their organs (Medvedev 2012). To resist the gravitational force, they form strong mechanical tissues. Nonetheless, the plasticity of their development allows plants to go through the complete life cycle from seed to seed even on board of the International Space Station where they are exposed to weightlessness, or microgravity (Vandenbrink and Kiss 2016). Plants grown in space are generally similar to those grown on Earth. Their stems and roots elongate and develop axial symmetry, and leaves are dorsiventral. Thus, the shape of plant cells is generally preserved, and the direction of growth is focussed on sources of light, water, nutrients, oxygen, and carbon dioxide. And yet plants grown in space differ in many of the studied parameters from those on Earth. Their roots exhibit waving and skewing behaviour (Paul *et al*. 2012) and enhanced phototropic reactions (Kiss *et al*. 2012). Changes in the transcriptome and proteome show signs of stress responses (Paul *et al*. 2017; Frolov *et al*. 2018). Plant development in space is usually delayed, growth is impaired (Manzano *et al*. 2018) and productivity is reduced (De Micco *et al*. 2014).

Conditions of microgravity are effectively modelled by rotation of plants in two-axial (2A) clinostats or random positioning machines (RPMs), which rotate plants simultaneously around two perpendicular axes thus effectively averaging gravity vector to zero over time and allow plants to grow randomly as achieved in spaceflight (Kiss *et al*. 2019). The growth habits of plants in 2A clinostats and RPMs are similar to those in space (Paul

et al. 2012). Kraft *et al.* (2000) confirmed this thesis by comparing the position of amyloplasts in columella of *Arabidopsis* seedlings that were rotated around two axes with those that were exposed to true microgravity during spaceflight. It has been shown that the arrangement of amyloplasts in the columella seedlings during seedlings rotation in the RPM becomes as dispersed as in space flight conditions. The obvious drawback of this approach is that disoriented plants still have to uphold their weight. An equally obvious advantage of ground-based microgravity simulation is that it provides the opportunity to avoid several factors that inevitably act on board of space stations: cosmic radiation, confined volume, lack of convection, and higher content of ethylene (Vandenbrink and Kiss 2016).

Plant responses to gravity and to simulated microgravity are regulated at the cellular and molecular levels by metabolome and proteome adjustments (Vandenbrink and Kiss 2016; Frolov *et al*. 2018; Chantseva *et al*. 2019). Presumably, it is the cytoskeleton that determines the direction of both cell division and cell expansion. Its orientation is set by mechanisms of self-organisation, as well as the external directional cues. Still, our notion on the cytoskeleton behaviour in microgravity is limited to data on the cortical microtubules in shoots (Soga *et al*. 2018), and information on the actin cytoskeleton behaviour is not available at all. In this study, we examine the organisation and quantify rearrangements of actin microfilaments (MF) and tubulin microtubules (MT) that occur in elongating cells of roots and hypocotyls of *Arabidopsis* seedlings in response to 2A clinorotation.

Materials and methods

Plant material and growth conditions

Experiments were performed using seedlings of transgenic *Arabidopsis thaliana* (L.) Heynh, ecotype Col-0, transformed with constructs for imaging of cytoskeleton *in vivo*. For actin cytoskeleton imaging in roots and shoots, we used *GFP-fABD2* plants that constitutively expressed GFP fused with a second (C-terminal) actin-binding domain of fimbrin 1 (fABD2) (Voigt *et al*. 2005), and *Lifeact-Venus* plants that constitutively express a short actin-binding Lifeact peptide, fused with Venus fluorescent reporter (Riedl *et al*. 2008). For live imaging of microtubules, we used *GFP-MAP4* construct to study roots (Mathur and Chua 2000), and *GFP-TUA6* to study hypocotyls (Ueda *et al*. 1999). Plants were grown in sterile conditions on the surface of solidified half-strength Murashige−Skoog nutrient medium (MS/2; Duchefa, the Netherlands) containing 1% (mass/vol.) sucrose (Ecros, Russia) and 0.35% (mass/vol.) phytagel (Sigma-Aldrich, USA) in 60 mm Petri plates (Eppendorf, Germany). After stratification (2 days at 4°C), plates were placed either vertically or mounted in a continuously rotating 2A clinostat for 5 or 9 days in the MLR-351 climate chamber (Panasonic, Japan) at 20°C with a 16h/8 h light/dark cycle and at 100 $\mu molm^{-2}s^{-1}$ illuminance provided by FL40SS-W/37 fluorescent lamps.

Vertical growth, clinorotation, and gravistimulation

We used seedlings grown in vertical plates, in a 2A clinostat, and those subjected to gravistimulation by replacement from the 2A clinostat to a vertical position for 30 min. We used a custom-made 2A clinostat that allowed simultaneous rotation of Petri plates around two orthogonal axes at 2.5 rpm frequency (Frolov *et al*. 2018) (see Supplementary Movie 1).

Seedling measurements

Digital images of plants were taken by Sony α7R3 camera equipped with Canon EF 180 mm f/3.5 L Macro USM lens and mounted on focusing rails. Images were processed in ImageJ (ver. 1.52p) for measurements. Root length was measured by tracing the root with the 'segmented line' tool from the root collar along the root to the root tip. The same approach was applied to measure hypocotyl length. Root curvature (dimensionless units) was calculated as the root length divided by the length of the straight line drawn between the root collar and the root tip. Root angle was measured in the root tip–root collar line and the vertical line drawn on a plate. In each experiment, 12–15 seedlings were examined.

Cytoskeleton visualisation

Confocal microscopy experiments were carried out using a Leica TCS SP5 MP inverted confocal laser scanning microscope (Leica Microsystems, Germany), equipped with a 40× objective lens with numerical aperture of 1.3 and oil immersion. Reporter protein fluorescence was induced with a 488 nm argon laser (20–35% power), and emission was recorded in the range of 510–550 nm with gain 80 ÷ 250 for GFP reporter lines (*GFP-fABD2*, *GFP-MAP4*, *GFP-TUA6*) and with gain 35 for *Lifeact-Venus*. Z-stacks of 14 to 16 optical sections (280 × 280 μm) were made at 2.5 μm intervals.

Analysis of cytoskeleton organisation

We analysed actin microfilaments (MF) and tubulin microtubules (MT) visualised in the root distal elongation zone (DEZ) and the middle part of hypocotyls using 5-day-old seedlings. Using Leica Application Suite 2010, confocal z-stacks of optical sections were divided into two sub-stacks corresponding to the stele or cortex section, then maximal projections were made and used for the subsequent analysis. Actin MF detection and analysis of their angular distribution were performed automatically using the Microfilament Analyzer software (Jacques *et al*. 2013) with the following settings: contrast 1.5, min length 10 px, diameter 1 px, detection threshold 3×, angular step 3°. Same settings were applied to MT analysis. Each sample represents at least 15 seedlings, 10 cells per seedling. We determined the frequency of MFs and MTs within the range of 0–30° (longitudinal), 30–60° (oblique), 60–90° (transverse) to the longitudinal root axis. The overall organisation of MFs or MTs was defined as 'scattered' if there was no predominant fraction among longitudinal, oblique or transverse MFs/MTs. Data on histograms show the percentage of longitudinal, oblique and transverse ones in confocal images. Density of MFs and MTs was calculated based on Microfilament Analyzer output as the number of MF or MT linear segments per μm^2 of cell projection.

Hydrogen peroxide assay

H_2O_2 was quantified with FOX reagent (Gay and Gebicki 2000) according to the following procedure. Approximately 27–30 9-day-old seedlings were homogenised at 4°C with 1 mL of 0.3 M perchloric acid and centrifuged at 15000*g* for 10 min. A volume of 72 µL of 1M K-phosphate buffer (pH 6.0) was added to 800 µL of supernatant, and the pH was adjusted to 6.0 with 1N KOH. To remove ascorbic acid from the sample, 10 µL of ascorbate oxidase (Sigma-Aldrich ascorbate oxidase from Cucurbita, 1–3 kU mg^{-1} protein) solution (0.1 U μL^{-1}) in 50 mM K-phosphate buffer (pH 6.0) was added. After 5 min, two aliquots of 500 µL were taken. To one aliquot, 10 µL of catalase (Sigma-Aldrich catalase from bovine liver, 2–5 kU mg^{-1} protein) solution (4 U μL^{-1}) in the same buffer was added; to the other aliquot, an equal amount of the buffer was added. After 10 min, 510 µL of FOX reagent was added to each sample. After 30–40 min, the optical density was measured at 560 nm with NanoPhotometer P300 (Implen, Germany). The composition of FOX reagent was: 200 mM sorbitol (Sigma-Aldrich), 50 mM sulfuric acid, 0.2 mM xylenol orange (Sigma-Aldrich), 0.5 mM ferric sulfate, 0.5 mM ammonium sulfate in water solution. Hydrogen peroxide content was calculated as the difference in optical densities between aliquots with and without catalase using specific extinction of H_2O_2 (~0.08 μM^{-1} cm^{-1} determined by calibration curve). All the inorganic reagents mentioned above were purchased from Ecros, Russia.

Statistical data analysis

All experiments were performed with at least three replicates. Statistical data analysis was performed in Microsoft Excel and significance was estimated using Student's *t*-test. Data are mean values with standard errors.

Results

Microgravity modelling by 2A clinorotation induces changes in the development of Arabidopsis *seedlings*

Vertically grown 5-day-old *Arabidopsis* seedlings exhibited normally developed roots, hypocotyls and cotyledons (Fig. 1*a–d*), but the length of roots and hypocotyls varied among studied transgenic lines. *GFP-TUA6* and *GFP-fABD2* hypocotyls were 20–24% shorter (Fig. 2*a*), while *GFP-TUA6* roots were 24% longer than wild-type ones (Fig. 2*b*). Root curvature and root angle were consistent within studied lines with values from 1.02 to 1.05 (dimensionless units) and 8.5 ± 2.3°, respectively (Fig. 2*c*, *d*).

Microgravity modelling by 2A clinorotation induced several changes in seedlings phenotype. The most noticeable change was in the mode of the root growth (Figs 1, 2*b–d*). The roots showed a significant decrease in length and an increase in skewing under 2A clinorotation (Fig. 2*b*, *d*). Their deviation from the conventional vertical lines drawn on each plate reached 140°, with a tendency to the left-handed skewing when observed from above (Figs 1, 2*d*).

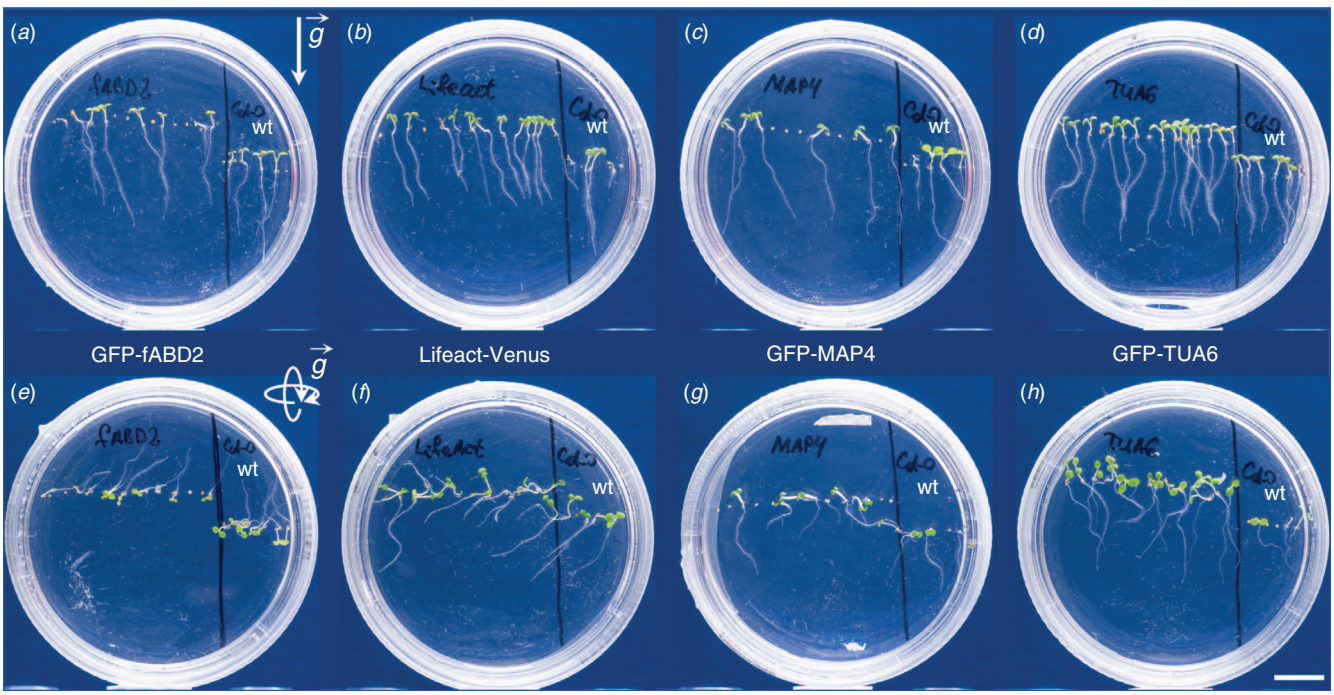

Fig. 1. Vertically grown (*a–d*) and 2A clinorotated (*e–h*) seedlings of 5-day-old *A. thaliana* as seen from the top of plates. Each plate held wild-type seedlings (Col-0), to the right of black marker line, and one of the following transgenic lines used for *in vivo* cytoskeleton visualisation. (*a*, *e*) *GFP-fABD2* (actin microfilaments), (*b*, *f*) *Lifeact-Venus* (actin microfilaments), (*c*, *g*) *GFP-MAP4* (microtubules in roots), (*d*, *h*) *GFP-TUA6* (microtubules in shoots). Scale bar, 10 mm.

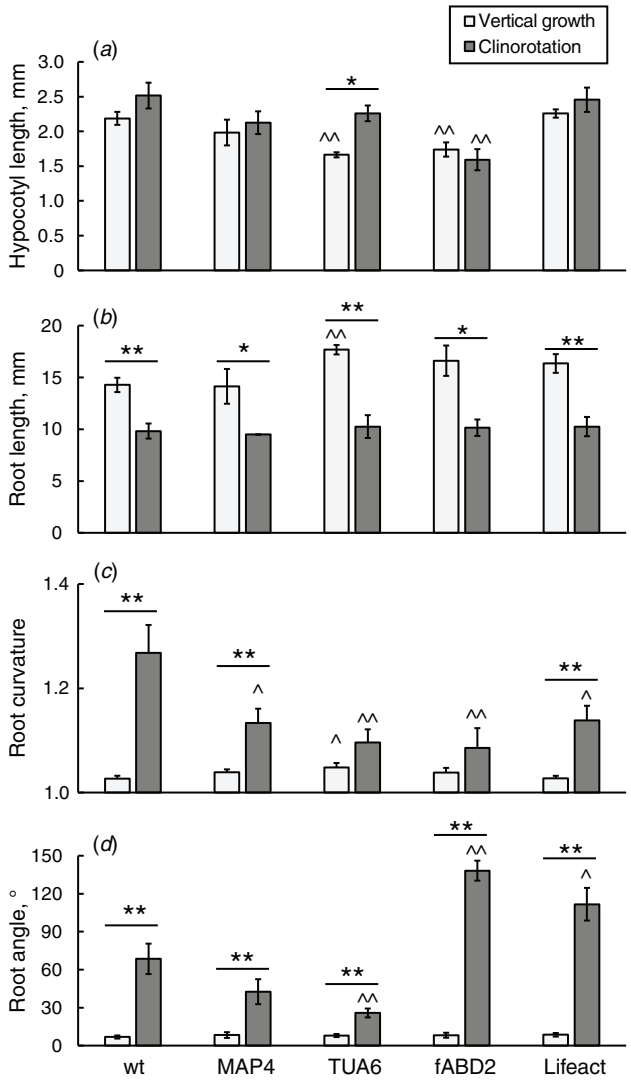

Fig. 2. Morphology analysis of 5-day-old vertically grown and 2A clinorotated seedlings of wild-type *A. thaliana* (Col-0) and transgenic lines used for cytoskeleton *in vivo* visualisation (*GFP-fABD2*, *Lifeact-Venus*, *GFP-MAP4*, and *GFP-TUA6*). Measured parameters are (*a*) hypocotyl length, (*b*) root length, (*c*) root curvature (dimensionless units) and (*d*) angle between the root tip and the root collar line vs vertical line. The data are mean ± s.e. from four independent experiments; 12–15 seedlings were examined in each experiment. Asterisks (*) and circumflex (^) symbols indicate statistical significance for the difference between vertically grown and clinorotated plants, and between the wild-type and the transgenic line, respectively (Student's *t*-test). *, $P < 0.05$; **, $P < 0.01$.

The roots exhibited wavy pattern of growth, which was significant in wild-type, *GFP-MAP4* and *Lifeact-Venus* seedlings (Fig. 2*c*). It should be noted that the root curvature of all transgenic lines was less than that of wild-type seedlings. Hypocotyls of clinorotated seedlings were positioned under various angles to the vertical, and *GFP-TUA6* hypocotyls also exhibited a significant increase in the length (Fig. 2*a*; $P < 0.05$).

Table 1. The effect of long-term (9 days) and short-term (24 h) 2A clinorotation on the *Arabidopsis* seedlings biomass and hydrogen peroxide content

The data are mean ± s.e. from three independent experiments

Seedling orientation	Biomass (FW; mg)	H_2O_2 content (nmol g^{-1} FW)
Vertical growth	4.5 ± 0.4	32 ± 3
Clinorotation after 9 days	3.1 ± 0.3	30 ± 3
Clinorotation for the 9th day (24 h)	3.1 ± 0.3	50 ± 5

Hydrogen peroxide accumulation in seedlings under 2A clinorotation

The development of *Arabidopsis* seedlings under continuous 2A clinorotation showed signs of stress. In 5-day-old seedlings, that was manifested in the inhibition of root growth (Fig. 2*b*). In 9-day-old seedlings, that also led to the inhibition of leaf development and to a significant decrease in the fresh weight of seedlings (Table 1). H_2O_2 level was quantified in seedlings as one of the integral indicators of stress. Under continuous 2A clinorotation for 9 days, seedlings did not exhibit differences in H_2O_2 content with those grown in vertical plates. However, oxidative stress accompanied by growth inhibition was revealed in 8-day-old control seedlings that were subjected to 2A clinorotation for the following 24 h (for the 9th day).

2A clinorotation results in more 'scattered' organisation of the actin cytoskeleton in Arabidopsis *seedlings*

We have studied actin cytoskeleton *in vivo* in 5-day-old seedlings using two different transgenic marker lines proven to be effective for MF visualisation: *GFP-fABD2* and *Lifeact-Venus*. As shown earlier (Pozhvanov *et al*. 2016), MFs had a predominantly longitudinal orientation in the cortex and stele of the root DEZ (Figs 3*a*, *d*, 4*a*). In hypocotyls, the fraction of longitudinal MFs was also predominant (Figs 3*j*, *m*, 4*d*). In *Lifeact-Venus* seedlings, a fine MF network was revealed better than in *GFP-fABD2* (Fig. 3). Seedlings of transgenic lines also displayed differences in the MF orientation although they were not statistically significant (Fig. 4). In *Lifeact-Venus* seedlings, the longitudinal MF fraction was smaller, and the oblique MF fraction was larger than in *GFP-fABD2* seedlings. Transverse MFs were minor in both *GFP-fABD2* and *Lifeact-Venus* seedlings.

Under 2A clinorotation, *GFP-fABD2* seedlings showed an increase in MF density in roots (Fig. 5*a*) and a decrease in MF density in hypocotyls (Fig. 5*b*). In *Lifeact-Venus* seedlings, a decrease in MF density was observed in both roots and hypocotyls (Fig. 5*a*, *b*).

The effect of 2A clinorotation on MF orientation was most pronounced in *GFP-fABD2* seedlings. In their root DEZ cortex, the proportion of longitudinal MFs was significantly reduced: 40% vs 60% in seedlings grown on vertical plates (Fig. 4*a*, *b*; $P < 0.01$). Thus, due to the decrease of longitudinal MF fraction and the corresponding increase of oblique and transverse MF fractions, the orientation of MFs in the DEZ cortex under 2A clinorotation became 'scattered'.

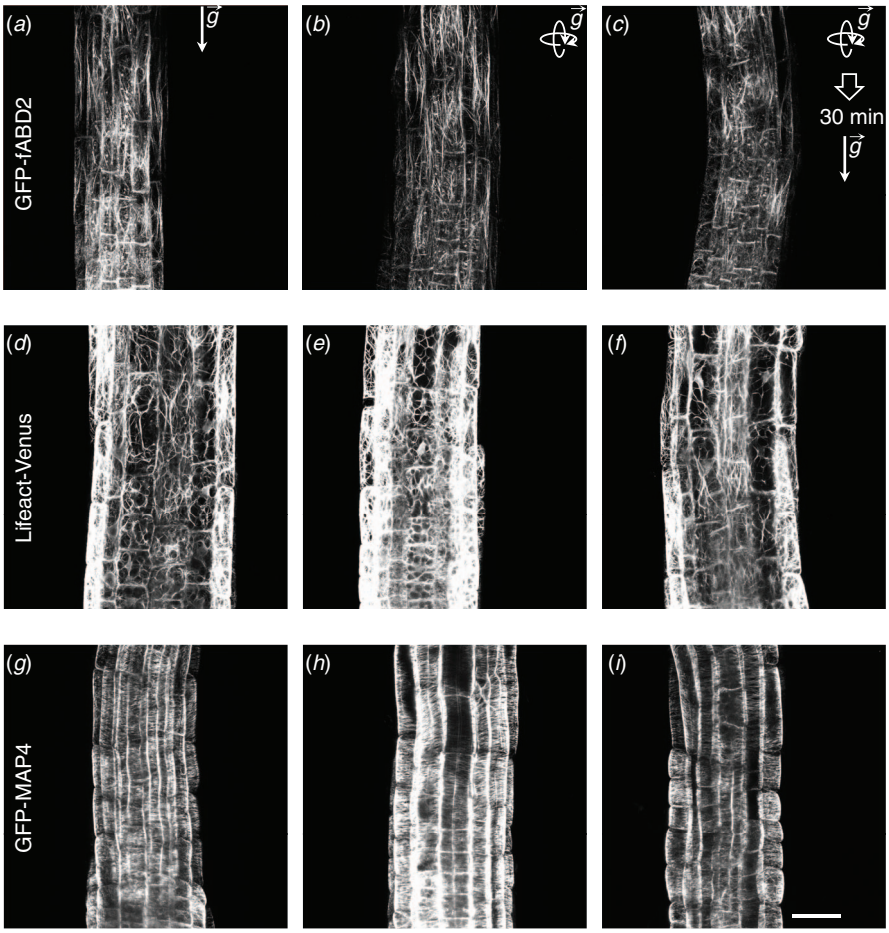

Fig. 3. Visualisation of microfilaments and microtubules in roots and hypocotyls of 5-day-old *A. thaliana* transgenic seedlings. Cytoskeleton was visualised *in vivo* in the root distal elongation zone and in elongating hypocotyls of seedlings grown vertically (*a*, *d*, *g*, *j*, *m*, *p*), in the two-axial clinostat (*b*, *e*, *h*, *k*, *n*, *q*), or 30 min in the vertical orientation after 5 days of clinorotation (*g*, *h*, *i*, *l*, *o*, *r*). (*a–c*) Actin cytoskeleton in *GFP-FABD2* roots, (*d–f*) actin cytoskeleton in *Lifeact-Venus* roots, (*g–i*) microtubules in *GFP-MAP4* roots, (*j–g*) actin cytoskeleton in *GFP-FABD2* hypocotyls, (*m–o*) actin cytoskeleton in *Lifeact-Venus* hypocotyls, and (*p–r*) microtubules in *GFP-TUA6* hypocotyls. Maximal intensity projections of 6–8 confocal optical sections through root or hypocotyl cortex are shown. Figures demonstrate typical images from experimental series (at least 15 seedlings were examined in either experiment). Scale bar, 50 μm.

In *GFP-fABD2* hypocotyls, the fraction of longitudinal MFs was also significantly lower in conditions of 2A clinorotation: 55–60% vs 65–70% in vertical control (Fig. 4*d*, *e*; $P < 0.05$). In contrast to the roots, these effects were observed both in the cortex and in the stele.

Visualisation of MFs in *Lifeact-Venus* seedlings gave different results. Under 2A clinorotation, the longitudinal MF fraction in the cortex of the root DEZ became statistically indistinguishable from the fraction of transverse MFs (42 ± 14% vs 15 ± 5%), whereas in vertically grown seedlings, the differences between these fractions were statistically significant: 45 ± 5% vs 14 ± 3% (Fig. 4*a*, *b*; $P < 0.05$). In the *Lifeact-Venus* hypocotyls, no changes were detected in the MF orientation under conditions of 2A clinorotation.

In *GFP-fABD2* marker line, microgravity modelling by 2A clinorotation resulted in more ‘scattered’ orientation of MFs in the elongating cells of roots and hypocotyls. To check whether constant gravity vector could promptly adjust actin cytoskeleton organisation, we performed an experiment where continuously clinorotated seedlings were subjected to their first in-a-lifetime gravistimulation, a vertical placement. We have previously shown that gravistimulation by 90° rotation of plants with respect to the gravity vector resulted in actin MF rearrangement within 20–30 min (Pozhvanov *et al.* 2016); therefore, the same 30 min exposure to gravity was chosen for this experiment as well. Remarkably, the initial gravistimulation of 2A clinorotated plants resulted in fast actin cytoskeleton rearrangement in roots, which organisation became similar to that of vertically grown

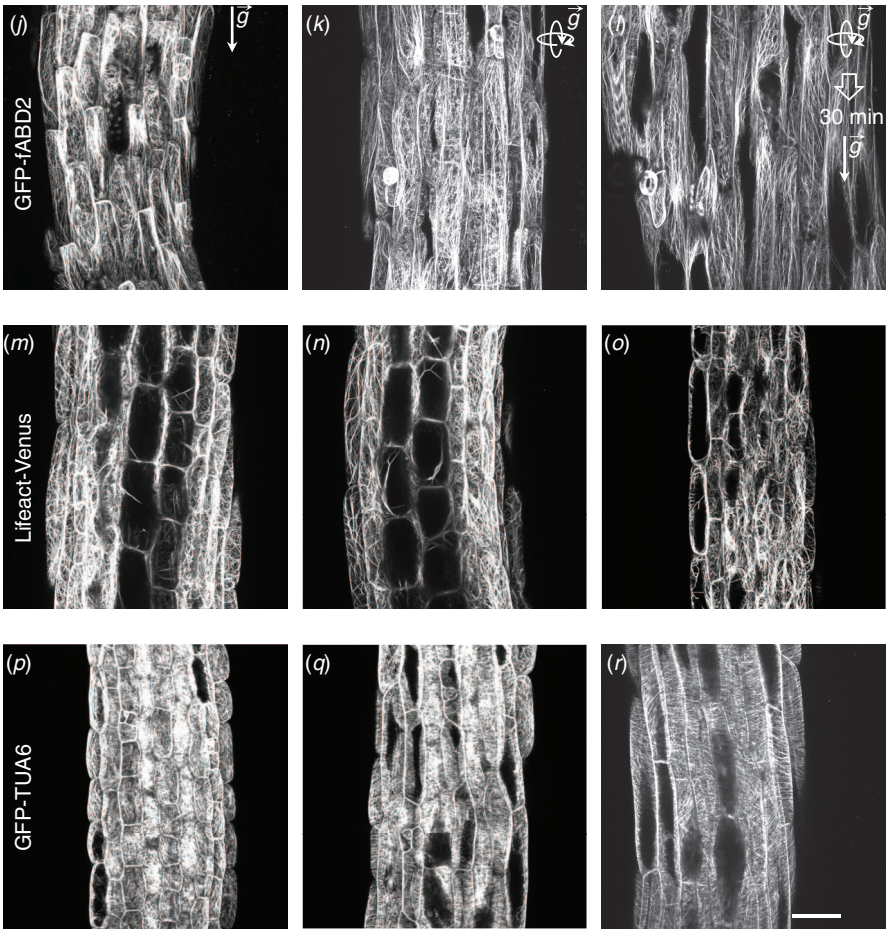

Fig. 3. (*Continued*)

seedlings (Fig. 3*c*, *f*). In *GFP-fABD2* and in *Lifeact-Venus* root cortex, longitudinal MFs became dominant again (Fig. 4*c*). MF density response in roots of seedlings placed vertically after 2A clinorotation presumably showed a lag except for stele of *GFP-fABD2* roots that showed similar distributions as the controls (Fig. 5*a*). In *GFP-fABD2* hypocotyls, MF orientation and density also 'restored' to the control one (Figs 3*l*, *o*, 4*f*, 5*b*).

2A clinorotation has minor effect on the orientation of microtubules in Arabidopsis *seedlings*

To analyse the orientation of the MTs in the roots, we used only *GFP-MAP4* seedlings (Fig. 3*g–i*) because GFP-TUA6 fusion proteins are not fully incorporated into cortical microtubules in root cells (Abe and Hashimoto 2005). Under conditions of vertical growth, the ratio of longitudinal, oblique and transverse MTs in the DEZ cortex was 28:37:35 (Fig. 6*a*). Under 2A clinorotation, the ratio of these fractions was 30:33:37 (Fig. 6*b*). Thus, the fraction of transverse MTs slightly increased. After 30 min in the vertical position, the ratio of MT fractions also shifted towards transverse (Fig. 6*c*). In the DEZ stele, there were no changes in the orientation of the MTs under 2A clinorotation.

GFP-TUA6 seedlings better suited for MT visualisation in hypocotyls (Fig. 3*p–r*). In the cortex of hypocotyls, longitudinal MTs prevailed, and the ratio of longitudinal, oblique and transverse MT was 46:36:18 (Fig. 6*a*). Under 2A clinorotation, this ratio was 43:37:20 (Fig. 6*b*). Thus, transverse MTs fraction exhibited a tendency to increase at the expense of longitudinal MTs. This trend was the same in the stele, where the ratio of these fractions in the vertical control was 44:38:18 and shifted to 41:38:21 under 2A clinorotation. Thirty min after the clinorotation was stopped and seedlings were exposed to a constant gravity vector, these effects persisted and even increased further (Fig. 6*c*). MT density showed very moderate response to 2A clinorotation (Fig. 5*c*, *d*). To conclude, 2A clinorotation imposed a minor effect on the orientation of MTs, which on the whole was expressed in a decrease in the longitudinal and oblique MT fractions and an increase in the fraction of transverse MTs.

Discussion

There are many studies focussed on the growth pattern of *Arabidopsis* seedlings in real microgravity in space and in microgravity modelled with ground-based facilities.

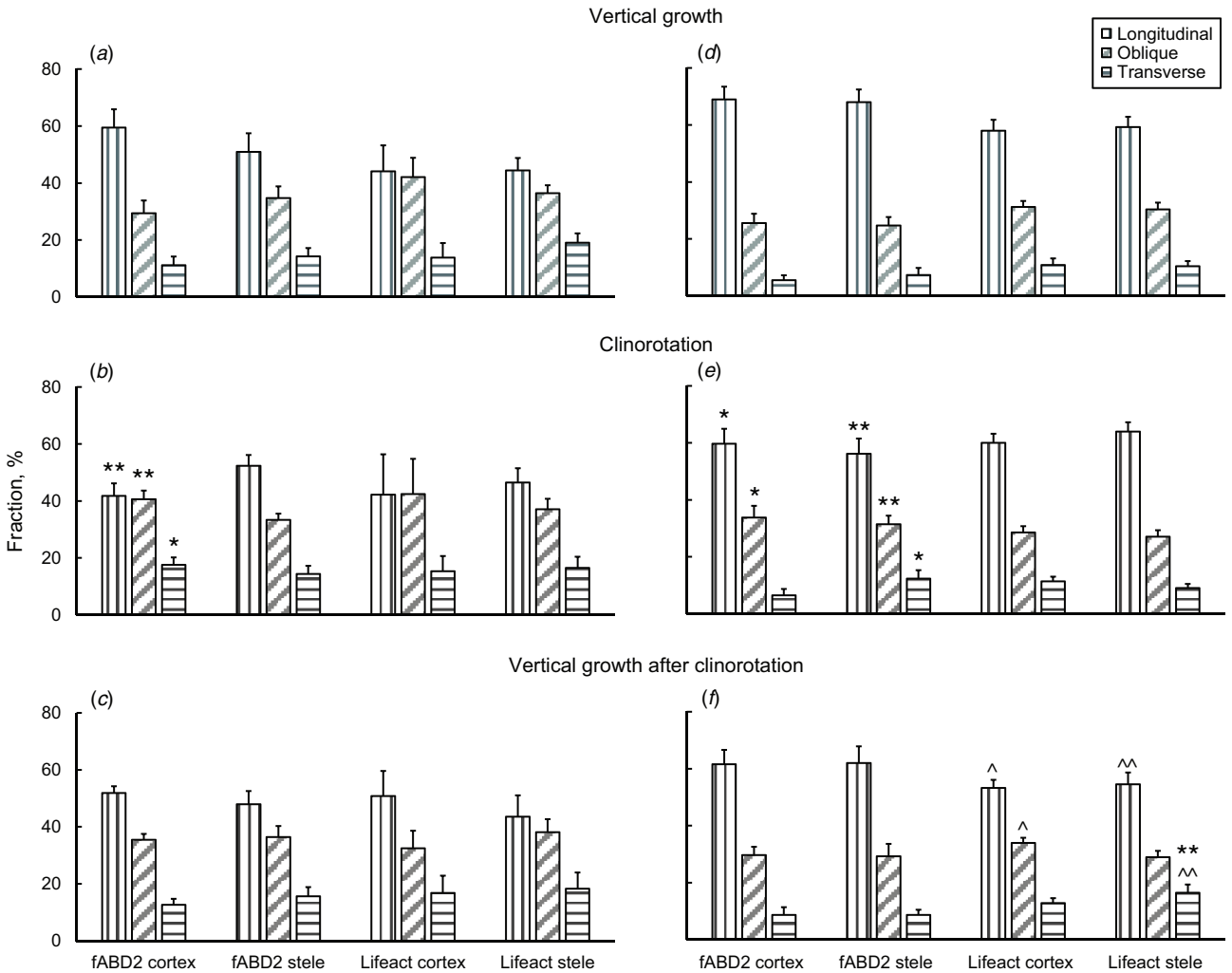

Fig. 4. Microfilament orientation in cortex and stele of root distal elongation zone (*a*, *b*, *c*), and in elongating hypocotyls (*d*, *e*, *f*) of 5-day-old *A. thaliana GFP-fABD2* and *Lifeact-Venus* seedlings grown vertically (*a*, *d*), in the two-axial clinostat (*b*, *e*), or 30 min in the vertical orientation after 5 days of clinorotation (*c*, *f*). Microfilaments were classified as longitudinal, oblique or transverse depending on the angle they made with respect to the root apical-basal axis. The data are mean ± s.e. from four independent experiments. At least 15 seedlings were examined in each experiment, 10 cells per seedling. Asterisks (*) and circumflex (^) symbols show that the values are significantly different from those of the vertically oriented or clinorotated seedlings, respectively (Student's *t*-test). *, $P < 0.05$; **, $P < 0.01$.

Obviously, there are some differences between the results obtained. In our experiments, we observed that under 2A clinorotation, *Arabidopsis* seedlings had shorter roots, longer hypocotyls, and lower biomass (Figs 1, 2; Table 1). Inhibition of root elongation was also observed by Paul *et al*. (2012) in experiments carried out on the International Space Station. However, in other studies, flight-grown roots had the same length as the ground-grown ones (Kiss *et al*. 2012; Nakashima *et al*. 2014; Paul *et al*. 2017). Besides, it was observed using RPM that the effect of microgravity on root elongation depends on the *Arabidopsis* ecotype (Piconese *et al*. 2003).

The elongation of *Arabidopsis* hypocotyls in space also changed in different ways, it was either retarded (Paul *et al*. 2012) or accelerated (Soga *et al*. 2018). Data on phenotypes of other species seedlings are equally ambiguous. For instance, rapeseed (*Brassica napus* L.) germination and the primary root elongation were accelerated under 2A clinorotation (Frolov *et al*. 2018; Chantseva *et al*. 2019), while growth of rice (*Oryza sativa* L.) shoots was slightly retarded in space (Wakabayashi *et al*. 2017). Obviously, the discrepancies mentioned above are due to the fact that gravity is not the main factor determining the growth rate. To a great extent, plant growth depends on the composition of the growing medium, light, hardware and spaceflight conditions. The role of these factors in microgravity may be altered. For example, in space, *Arabidopsis* hypocotyls and roots demonstrate significantly stronger phototropic responses (Kiss *et al*. 2012).

Plants are able to withstand microgravity. However, there are many indications that microgravity causes stress responses. In conditions of real and modelled microgravity, adjustments in the transcriptome and proteome were mostly associated with

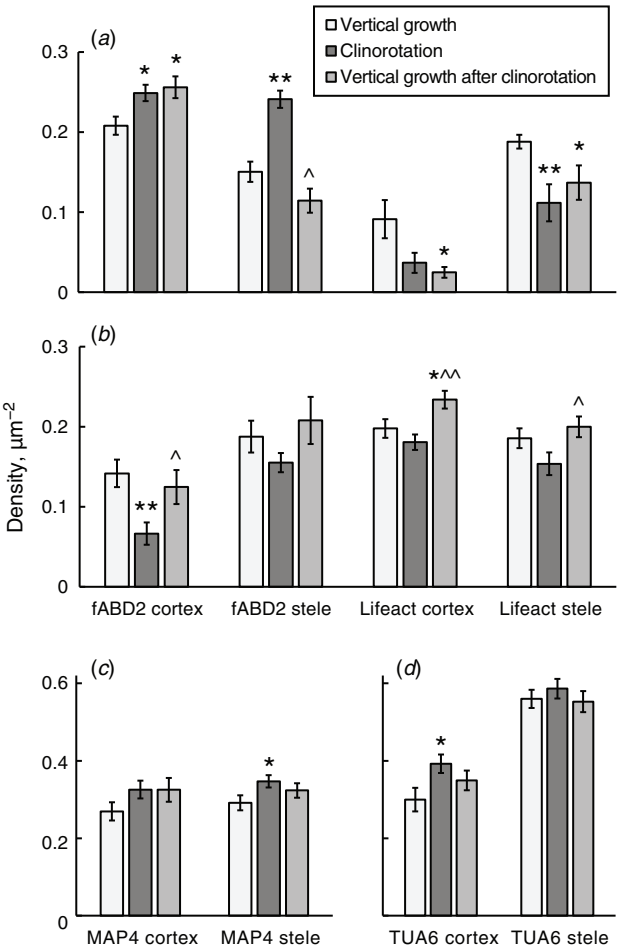

Fig. 5. Density of microfilaments (MFs) (*a*, *b*) and microtubules (MTs) (*c*, *d*) in cortex and stele of root distal elongation zone (*a*, *c*), and in elongating hypocotyls (*b*, *d*) of 5-day-old *A. thaliana GFP-fABD2*, *Lifeact-Venus*, *GFP-MAP4* and *GFP-TUA6* seedlings grown vertically, in the two-axial clinostat, or 30 min in the vertical orientation after 5 days of clinorotation. MF and MT density is expressed as the number of their linear segments per μm^2 of cell projection. The data are mean ± s.e. from four independent experiments. At least 15 seedlings were examined in each experiment, 10 cells per seedling. Asterisks (*) and circumflex (^) symbols show that the values are significantly different from those of the vertically grown or clinorotated seedlings, respectively (Student's *t*-test). *, $P < 0.05$; **, $P < 0.01$.

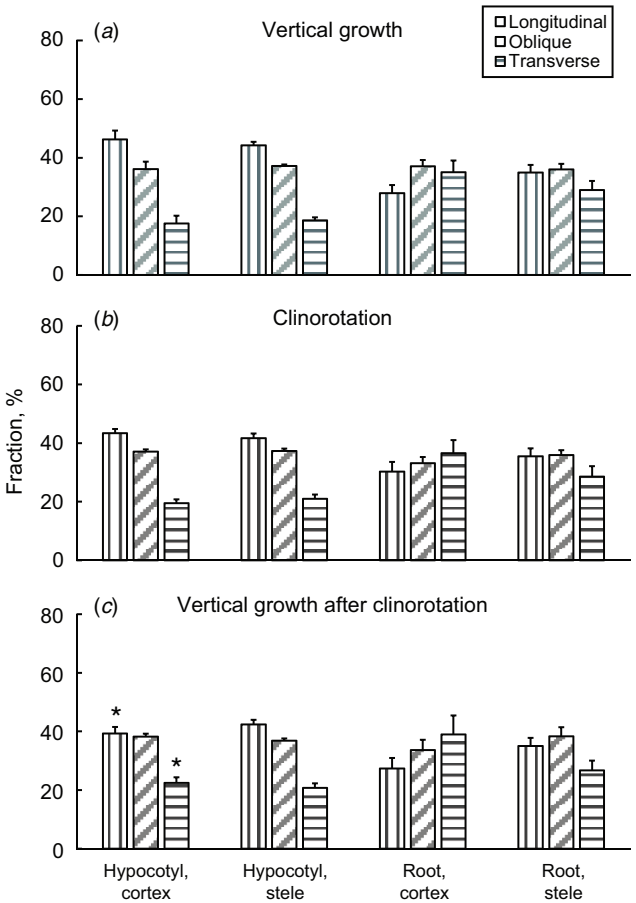

Fig. 6. Tubulin cytoskeleton orientation in stele and cortex of 5-day-old *A. thaliana GFP-TUA6* hypocotyls and *GFP-MAP4* roots grown vertically (*a*), during continuous clinorotation (*b*), or within 30 min of their initial vertical placement after continuous 2A clinorotation (*c*). Microtubules were classified as longitudinal, oblique or transverse depending on the angle they made with respect to the apical-basal axis. The data are mean ± s.e. from four independent experiments. At least 15 seedlings were examined in each experiment, 10 cells per seedling. Asterisks (*) indicate values that are significantly different from those of the vertically oriented plants (Student's *t*-test). *, $P < 0.05$.

stress responses, phytohormone signalling, and cell wall remodelling (Paul *et al*. 2017; Frolov *et al*. 2018). Our data on the dynamics of hydrogen peroxide content in seedlings also indicate that there was an oxidative stress under 2A clinorotation (Table 1).

Under 2A clinorotation, the curvature of roots and their deviation from the vertical line, with a tendency to left-handedness, significantly increased (Figs 1, 2). Increased waving and skewing of *Arabidopsis* roots were also observed in RPMs (Piconese *et al*. 2003) and in space (Paul *et al*. 2012; Nakashima *et al*. 2014). The waving and skewing pattern of *Arabidopsis* root growth was also described in the conditions of Earth's gravity. It strongly depends on the position of Petri plates (Roy and Bassham 2014), composition and density of the growth medium (Schultz *et al*. 2016), and *Arabidopsis* ecotype (Paul *et al*. 2012; Schultz *et al*. 2017).

The nature of root waving and skewing, as well as a cause for the enhancement of these phenomena in microgravity, remain obscure. Nevertheless, the precise basis of these growth patterns is not well understood and both gravity and the contact between the medium and the root are probably the major players that result in these processes (Oliva and Dunand 2007). The traditional view that root waving and skewing are interrelated phenomena that are the combined result of endogenous circumnutations of the growing root tip, touch and gravity responses, was recently revised (Roy and Bassham 2014). The fact that root waving and skewing are observed and even increased in weightlessness proves that gravitropism is not a compulsory part of these phenomena. In addition, using different plates orientation and different ecotypes of

Arabidopsis, these phenomena were separated (Schultz *et al*. 2016). Gene expression patterns associated with waving and skewing are different (Schultz *et al*. 2017). Using wild-type plants and several transgenic lines, we also found that while both root waving and skewing increased in microgravity, the correlation between them was weak. For example, the most pronounced waving pattern of root growth was demonstrated by wild-type plants, and the strongest skewing was observed in transgenic lines (Figs 1, 2).

Root growth is the result of cell division in the meristem and subsequent cell extension in the elongation zone. In microgravity, the roots form a functional meristem similar to vertically oriented roots. However, a detailed cytological study showed that the balance between cell division and cell growth was disrupted under RPM conditions (Manzano *et al*. 2018). G2 stage became shorter, and cells entered mitosis before reaching their normal size.

The elongation of the plant axial organs and their tropistic movements are based on anisotropic cell extension, which is supported by the cytoskeleton and is closely related to the polar auxin transport. MFs exhibit mainly longitudinal orientation in the elongation zone of the primary root of *Arabidopsis* (Jacques *et al*. 2013; Pozhvanov *et al*. 2016), maize (*Zea mays* L.) and alfalfa (*Medicago sativa* L.) (de Bang *et al*. 2020). MFs were longitudinal in elongating maize coleoptiles where growth inhibition was accompanied by MF bundling, and auxin-induced growth acceleration, by MF debundling and transition to the finer filaments (Nick 2010). We also found MFs to have predominantly longitudinal orientation in the root DEZ and in the elongating hypocotyls of *Arabidopsis* (Fig. 3, 4).

In our experiments, root waving and skewing under clinorotation were also accompanied by an orientation of MFs in a scattered manner and changes in their density (Figs 3, 4, 5*a*). Previously we showed that the MF orientation became more scattered during gravitropic bending of *Arabidopsis* roots (Pozhvanov *et al*. 2016). A decrease in the density of MFs and their more scattered orientation also accompanied the brassinolide-dependent increase of the gravitropical bending of maize roots (de Bang *et al*. 2020). Brassinolide also increased maize root curvature in a clinostat (de Bang *et al*. 2020). Stronger root waving in space was observed in *act2–3 Arabidopsis* mutants with the impaired actin cytoskeleton (Nakashima *et al*. 2014). Interestingly, 'scattered' organisation of MFs which we found in *Arabidopsis* under 2A clinorotation, is very similar to MF response to ethylene treatment, when the fraction of longitudinal MFs decreased and fractions of oblique and transverse MFs increased (Pozhvanov *et al*. 2016).

The role of MFs in the growth pattern of roots and shoots is interpreted in terms of their participation in the polar auxin transport (Nick 2010; Blancaflor 2013), which depends on the localisation of the auxin efflux transport proteins belonging to PIN family. PIN proteins constantly circulate by vesicle traffic between the plasma membrane and endosomal compartments (Kleine-Vehn *et al*. 2011). The actin cytoskeleton participates in this vesicular transport. Presumably, the dense MF network and MF bundling reduce the rate of PIN transcytosis and slow down their relocation during the root gravitropic response (Blancaflor 2013). The assumption of crosstalk between the actin cytoskeleton and auxin signalling is employed to explain the nature of rhythmic fluctuations in the growth rate of maize coleoptiles (Nick 2010).

Visualisation of the auxin distribution in the *Arabidopsis* roots showed that in microgravity auxin was still concentrated in the root tip (Herranz *et al*. 2014; Ferl and Paul 2016). In RPMs, the auxin peak covered the whole root meristem, whereas under vertical growth, it was focussed in the quiescent centre and columella cells (Herranz *et al*. 2014). In space conditions, no differences were found in the distribution of auxin from the ground control (Ferl and Paul 2016). Data on the auxin signalling in shoots also indicate the absence of its major perturbations in microgravity. For example, the auxin content did not change in rice shoots under space conditions and there was only little change in the expression of auxin-responsive genes with the exception of several *AUX*/*IAA*, which were downregulated (Wakabayashi *et al*. 2017). In cucumber (*Cucumis sativus* L.) seedlings, the localisation of CsPIN1 in endoderm cells in the hypocotyl to root transition zone did not change in space conditions (Yamazaki *et al*. 2016). It is obvious that the polar auxin transport system operates under microgravity. The establishment of this system is apparently guided by mechanisms of self-organisation. Hence, the 'randomisation' of the actin cytoskeleton found in our experiments is most likely connected with the waving pattern of root growth in conditions of clinorotation.

To visualise MTs, we used 5-day-old *Arabidopsis* seedlings grown in light conditions. In these seedlings, hypocotyl elongation was approaching its termination (Le *et al*. 2005). Accordingly, the fraction of transverse MTs was only ~20% (Fig. 6). In rapidly elongating cells of the root DEZ, it was significantly higher, 30–35%. Under 2A clinorotation, roots and hypocotyls showed a tendency to increase the fraction of transverse MTs at the expense of longitudinal ones (Fig. 6).

In contrast to MFs, the role of MTs in the regulation of anisotropic growth is usually explained by MT influence on the orientation of cellulose microfibrils orientation, which in turn determines the anisotropy of cell wall extensibility. Cell walls are more extensible in the direction transverse to the orientation of cellulose microfibrils (Bidhendi and Geitmann 2016). The relationship between the cortical MT orientation and the rate of cell elongation has been studied in both roots and shoots. For example, in the *Arabidopsis* root elongation zone, cortical MT in the epidermis and cortex are mainly transverse, and upon the cessation of growth their orientation changes to longitudinal and oblique (Panteris *et al*. 2013). Root swelling and inhibition of root elongation under ethylene treatment was accompanied by MT reorientation from transverse to longitudinal within 60 min (Wang *et al*. 2018). The orientation of cortical MTs is very closely related to the elongation rate of *Arabidopsis* hypocotyls. In 2-day-old *Arabidopsis* seedlings, cell division in hypocotyls stops and their further elongation occurs only due to the cell extension growth (Gendreau *et al*. 1997). The rate and duration of hypocotyl elongation are much greater in the dark than under the light. In rapidly elongating dark-grown hypocotyls, the fraction of transverse MTs reached 70% (Liu *et al*. 2013).

Under illumination, growth was inhibited within 60 min, and the MTs were reoriented to the longitudinal direction (Liu *et al*. 2013). Correspondingly, auxin-induced elongation of *Arabidopsis* hypocotyl segments was accompanied by a rapid reorientation of MTs from longitudinal to transverse (Adamowski *et al*. 2019). Put together, the data above highlight the involvement of MTs into regulation of anisotropic growth. Surprisingly, mechanical restriction of anisotropic growth was reported to prevent reorientation of cortical MTs in gravistimulated azuki bean (*Vigna angularis* L.) epicotyls (Ikushima and Shimmen 2005).

There are reports of the effects of gravitation force on the orientation of MTs in *Arabidopsis* seedlings. Under hypergravity conditions (300*g*), elongation of *Arabidopsis* hypocotyls was inhibited, and MTs were reoriented from transverse to longitudinal (Matsumoto *et al*. 2010). Correspondingly, the acceleration of *Arabidopsis* hypocotyl elongation in space was accompanied by a sharp increase in transverse MTs (Soga *et al*. 2018). Thus, an increase in the fraction of transverse MTs may explain the greater length of hypocotyls under clinorotation conditions (Fig. 2*a*).

It is also tempting to suggest causal relationship between the transitory rise in H_2O_2 concentration (Table 1) and the pattern of seedlings growth and cytoskeleton. Actin is known to be very susceptible to redox regulation and oxidation which is well documented for mammal cells (Wilson *et al.* 2016). Some data are available for plants. For example, *Arabidopsis* plants dying under 23 mM 2,4-D treatment exhibit actin depolymerisation, which might be the consequence of its carbonylation and nitrosylation induced by increased intracellular level of H_2O_2 (Rodríguez-Serrano *et al.* 2014). Treatment with high concentrations of H_2O_2 (0.5–1 mM) causes almost complete arrest of *Arabidopsis* root growth, sharp rearrangements of the actin cytoskeleton (Du *et al.* 2020) as well as redistribution of auxin in the root tips due to PIN2 transcytosis inhibition (Zwiewka *et al.* 2019). It is obvious that in these cases, the damaging effect of ROS is manifested, which is not directly applicable to the moderate changes that we observed under microgravity modelling. It is well known that auxin transport inhibitors block root waving, and among the waving mutants are *wav5*/*aux1* and *wav6*/*pin2*, with impaired auxin transport (Oliva and Dunand 2007). Therefore, the transient increase in H_2O_2 that we detected after 24 h of clinorotation, is most likely of a signalling nature. Study of the H_2O_2 dynamics in the apoplast of *Arabidopsis* plants grown in RPM will help clarify this issue.

Conclusions

Microgravity is considered to be one of the main factors affecting plant development in space conditions. Microgravity modelling by 2A clinorotation is an effective approach to study the role of gravity vector on Earth. Continuous spatial disorientation of *Arabidopsis* seedlings acts as a stressor that was manifested in transient H_2O_2 accumulation, slower seedling development and biomass growth. Under 2A clinorotation, actin cytoskeleton arrangement was altered, and the roots became shorter, wavy and skewed. The data presented here suggest that the 'scattered' orientation of actin microfilaments could serve as the default one for plant development under microgravity modelling and is promptly converted to an 'longitudinal' orientation under the constant gravity vector exposure.

Conflicts of interest

The authors declare no conflicts of interest.

Declaration of funding

This research was supported by Russian Foundation for Basic Research (projects 17–04–00862 and 20–04–01041).

Acknowledgements

The research was performed using the equipment of Research Resource Centre of St-Petersburg State University 'Molecular and Cell Technologies'. The authors thank Yuri Shevtsov and Galina Smolikova (Faculty of Biology, St. Petersburg State University) for engineering and assembly of the 3D clinostat device. The authors also thank Prof. Kris Vissenberg from University of Antwerp for generously providing *Arabidopsis* reporter line seeds.

References

Abe T, Hashimoto T (2005) Altered microtubule dynamics by expression of modified α-tubulin protein causes right-handed helical growth in transgenic *Arabidopsis* plants. *The Plant Journal* **43**, 191–204. doi:10.1111/j.1365-313X.2005.02442.x

Adamowski M, Li L, Friml J (2019) Reorientation of cortical microtubule arrays in the hypocotyl of *Arabidopsis thaliana* is induced by the cell growth process and independent of auxin signaling. *International Journal of Molecular Sciences* **20**, 3337. doi:10.3390/ijms20133337

Bidhendi AJ, Geitmann A (2016) Relating the mechanics of the primary plant cell wall to morphogenesis. *Journal of Experimental Botany* **67**(2), 449–461. doi:10.1093/jxb/erv535

Blancaflor EB (2013) Regulation of plant gravity sensing and signaling by the actin cytoskeleton. *American Journal of Botany* **100**, 143–152. doi:10.3732/ajb.1200283

Chantseva V, Bilova T, Smolikova G, Frolov A, Medvedev S (2019) 3D-clinorotation induces specific alterations in metabolite profiles of germinating *Brassica napus* L. seeds. *Biological Communications* **64** (1), 55–74. doi:10.21638/spbu03.2019.107

de Bang L, Paez-Garcia A, Cannon AE, Chin S, Kolape J, Liao F, Sparks JA, Jiang Q, Blancaflor EB (2020) Brassinosteroids inhibit autotropic root straightening by modifying filamentous-actin organization and dynamics. *Frontiers in Plant Science* **11**, 5. doi:10.3389/fpls.2020.00005

De Micco V, De Pascale S, Paradiso R, Aronne G (2014) Microgravity effects on different stages of higher plant life cycle and completion of the seed-to-seed cycle. *Plant Biology* **16**, 31–38. doi:10.1111/plb.12098

Du M, Wang Y, Chen H, Han R (2020) Actin filaments mediated root growth inhibition by changing their distribution under UV-B and hydrogen peroxide exposure in *Arabidopsis*. *Biological Research* **53**, 54. doi:10.1186/s40659-020-00321-3

Ferl RJ, Paul A-L (2016) The effect of spaceflight on the gravity-sensing auxin gradient of roots: GFP reported gene microscopy on orbit. *NPJ Microgravity* **2**, 15023. doi:10.1038/npjmgrav.2015.23

Frolov A, Didio A, Ihling C, Chantzeva V, Grishina T, Hoehenwarter W, Sinz A, Smolikova G, Bilova T, Medvedev S (2018) The effect of simulated microgravity on *Brassica napus* seedling proteome. *Functional Plant Biology* **45**(4), 440–452. doi:10.1071/FP16378

Gay C, Gebicki JM (2000) A critical evaluation of the effect of sorbitol on the ferric-xylenol orange hydroperoxide assay. *Analytical Biochemistry* **284**, 217–220. doi:10.1006/abio.2000.4696

Gendreau E, Traas J, Demos T, Crandjean O, Caboche M, Hofte H (1997) Cellular basis of hypocotyl growth in *Arabidopsis thaliana*. *Plant Physiology* **114**(1), 295–305. doi:10.1104/pp.114.1.295

Herranz R, Valbuena MA, Youssef K, Medina FJ (2014) Mechanisms of disruption of meristematic competence by microgravity in *Arabidopsis* seedlings. *Plant Signaling & Behavior* **9**, e28289. doi:10.4161/psb.28289

Ikushima T, Shimmen T (2005) Mechano-sensitive orientation of cortical microtubules during gravitropism in azuki bean epicotyls. *Journal of Plant Research* **118**, 19–26. doi:10.1007/s10265-004-0189-8

Jacques E, Lewandowski M, Buytaert J, Fierens Y, Verbelen J-P, Vissenberg K (2013) Microfilament analyzer identifies actin network organizations in epidermal cells of *Arabidopsis thaliana* roots. *Plant Signaling & Behavior* **8**, e24821. doi:10.4161/psb.24821

Kiss JZ, Millar KDL, Edelmann RE (2012) Phototropism of *Arabidopsis thaliana* in microgravity and fractional gravity on the International Space Station. *Planta* **236**, 635–645. doi:10.1007/s00425-012-1633-y

Kiss JZ, Wolverton C, Wyatt SE, Hasenstein KH, van Loon JJWA (2019) Comparison of microgravity analogs to spaceflight in studies of plant growth and development. *Frontiers in Plant Science* **10**, 1577. doi:10.3389/fpls.2019.01577

Kleine-Vehn J, Wabnik K, Martinie're A, Łangowski Ł, Willig K, Naramoto S, Leitner J, Tanaka H, Jakobs S, Robert S, Luschnig C, Govaerts W, Hell SW, Runions J, Friml J (2011) Recycling, clustering, and endocytosis jointly maintain PIN auxin carrier polarity at the plasma membrane. *Molecular Systems Biology* **7**, 540. doi:10.1038/msb.2011.72

Kraft TFB, van Loon JJWA, Kiss JZ (2000) Plastid position in *Arabidopsis columella* cells is similar in microgravity and on a random-positioning machine. *Planta* **211**(3), 415–422. doi:10.1007/s004250000302

Le J, Vandenbussche F, De Cnodder T, Van Der Straeten D, Verbelen J-P (2005) Cell elongation and microtubule behavior in the *Arabidopsis* hypocotyl: responses to ethylene and auxin. *Journal of Plant Growth Regulation* **24**, 166–178. doi:10.1007/s00344-005-0044-8

Liu X, Qin T, Ma Q, Sun J, Liu Z, Yuan M, Mao T (2013) Light-regulated hypocotyl elongation involves proteasome-dependent degradation of the microtubule regulatory protein WDL3 in *Arabidopsis*. *The Plant Cell* **25**, 1740–1755. doi:10.1105/tpc.113.112789

Manzano A, Herranz R, den Toom LA, te Slaa S, Borst G, Visser M, Medina FJ, van Loon JJWA (2018) Novel, Moon and Mars, partial gravity simulation paradigms and their effects on the balance between cell growth and cell proliferation during early plant development. *npj Microgravity* **4**, 9. doi:10.1038/s41526-018-0041-4

Mathur J, Chua N-H (2000) Microtubule stabilization leads to growth reorientation in *Arabidopsis* trichomes. *The Plant Cell* **12**, 465–477. doi:10.1105/tpc.12.4.465

Matsumoto S, Kumasaki S, Soga K, Wakabayashi K, Hashimoto T, Hoson T (2010) Gravity-induced modifications to development in hypocotyls of *Arabidopsis* tubulin mutants. *Plant Physiology* **152**, 918–926. doi:10.1104/pp.109.147330

Medvedev SS (2012) Mechanisms and physiological role of polarity in plants. *Russian Journal of Plant Physiology* **59**(4), 502–514. doi:10.1134/S1021443712040085

Nakashima J, Liao F, Sparks JA, Tang Y, Blancaflor EB (2014) The actin cytoskeleton is a suppressor of the endogenous skewing behaviour of *Arabidopsis* primary roots in microgravity. *Plant Biology* **16**, 142–150. doi:10.1111/plb.12062

Nick P (2010) Probing the actin-auxin oscillator. *Plant Signaling & Behavior* **5**(2), 94–98. doi:10.4161/psb.5.2.10337

Oliva M, Dunand C (2007) Waving and skewing: how gravity and the surface of growth media affect root development in *Arabidopsis*. *New Phytologist* **176**(1), 37–43. doi:10.1111/j.1469-8137.2007.02184.x

Panteris E, Adamakis I-DS, Daras G, Hatzopoulos P, Rigas S (2013) Differential responsiveness of cortical microtubule orientation to suppression of cell expansion among the developmental zones of *Arabidopsis thaliana* root apex. *PLoS One* **8**(12), e82442. doi:10.1371/journal.pone.0082442

Paul A-L, Amalfitano CE, Ferl RJ (2012) Plant growth strategies are remodeled by spaceflight. *BMC Plant Biology* **12**, 232. doi:10.1186/1471-2229-12-232

Paul A-L, Sng NJ, Zupanska AK, Krishnamurthy A, Schultz ER, Ferl RJ (2017) Genetic dissection of the *Arabidopsis* spaceflight transcriptome: Are some responses dispensable for the physiological adaptation of plants to spaceflight? *PLoS One* **12**(6), e0180186. doi:10.1371/journal.pone.0180186

Piconese S, Tronelli G, Pippia P, Migliaccio F (2003) Chiral and non-chiral nutations in *Arabidopsis* roots grown on the random positioning machine. *Journal of Experimental Botany* **54**(389), 1909–1918. doi:10.1093/jxb/erg206

Pozhvanov GA, Gobova AE, Bankin MP, Medvedev SS, Vissenberg K (2016) Ethylene is involved in the actin cytoskeleton rearrangement during the root gravitropic response of *Arabidopsis thaliana*. *Russian Journal of Plant Physiology: a Comprehensive Russian Journal on Modern Phytophysiology* **63**(5), 587–596. doi:10.1134/S1021443716050095

Riedl J, Crevenna AH, Kessenbrock K, Yu JH, Neukirchen D, Bista M, Bradke F, Jenne D, Holak TA, Werb Z, Sixt M, Wedlich-Soldner R (2008) Lifeact: a versatile marker to visualize F-actin. *Nature Methods* **5**(7), 605–607. doi:10.1038/nmeth.1220

Rodríguez-Serrano M, Pazmiño DM, Sparkes I, Rochetti A, Hawes C, Romero-Puertas MC, Sandalio LM (2014) 2,4-Dichlorophenoxyacetic acid promotes S-nitrosylation and oxidation of actin affecting cytoskeleton and peroxisomal dynamics. *Journal of Experimental Botany* **65**(17), 4783–4793. doi:10.1093/jxb/eru237

Roy R, Bassham DC (2014) Root growth movements: Waving and skewing. *Plant Science* **221–222**, 42–47. doi:10.1016/j.plantsci.2014.01.007

Schultz ER, Paul A-L, Ferl RJ (2016) Root growth patterns and morphometric change based on the growth media. *Microgravity Science and Technology* **28**, 621–631. doi:10.1007/s12217-016-9514-9

Schultz ER, Zupanska AK, Sng NJ, Paul A-L, Ferl RJ (2017) Skewing in *Arabidopsis* roots involves disparate environmental signaling pathways. *BMC Plant Biology* **17**, 31. doi:10.1186/s12870-017-0975-9

Soga K, Yamazaki C, Kamada M, Tanigawa N, Kasahara H, Yano S, Kojo KH, Kutsuna N, Kato T, Hashimoto T*, et al*. (2018) Modification of growth anisotropy and cortical microtubule dynamics in *Arabidopsis* hypocotyls grown under microgravity conditions in space. *Physiologia Plantarum* **162**, 135–144. doi:10.1111/ppl.12640

Ueda K, Matsuyama T, Hashimoto T (1999) Visualization of microtubules in living cells of transgenic *Arabidopsis thaliana*. *Protoplasma* **206**(1–3), 201–206. doi:10.1007/BF01279267

Vandenbrink JP, Kiss JZ (2016) Space, the final frontier: A critical review of recent experiments performed in microgravity. *Plant Science* **243**, 115–119. doi:10.1016/j.plantsci.2015.11.004

Voigt B, Timmers ACJ, Šamaj J, Müller J, Baluška F, Menzel D (2005) GFP-FABD2 fusion construct allows in vivo visualization of the dynamic actin cytoskeleton in all cells of *Arabidopsis* seedlings. *European Journal of Cell Biology* **84**(6), 595–608. doi:10.1016/j.ejcb.2004.11.011

Wakabayashi K, Soga K, Hoson T, Kotake T, Kojima M, Sakakibara H, Yamazaki T, Higashibata A, Ishioka N, Shimazu T, Kamada M (2017) Persistence of plant hormone levels in rice shoots grown under microgravity conditions in space: its relationship to maintenance of

shoot growth. *Physiologia Plantarum* **161**, 285–293. doi:10.1111/ppl.12591

Wang Y, Ji Y, Fu Y, Guo H (2018) Ethylene-induced microtubule reorientation is essential for fast inhibition of root elongation in *Arabidopsis*. *Journal of Integrative Plant Biology* **60**(9), 864–877. doi:10.1111/jipb.12666

Wilson C, Terman JR, Gonzalez-Billault C, Ahmed G (2016) Actin filaments – a target for redox regulation. *Cytoskeleton* **73**(10), 577–595. doi:10.1002/cm.21315

Yamazaki C, Fujii N, Miyazawa Y, Kamada M, Kasahara H, Osada I, Shimazu T, Fusejima Y, Higashibata A, Yamazaki T, Ishioka N, Takahashi H (2016) The gravity-induced re-localization of auxin efflux carrier CsPIN1 in cucumber seedlings: spaceflight experiments for immunohistochemical microscopy. *npj Microgravity* **2**, 16030. doi:10.1038/npjmgrav.2016.30

Zwiewka M, Bielach A, Tamizhselvan P, Madhavan S, Ryad EE, Tan S, Hrtyan M, Dobrev P, Vanková R, Friml J, Tognetti VB (2019) Root adaptation to H_2O_2-induced oxidative stress by ARF-GEF BEN1- and cytoskeleton-mediated PIN2 trafficking. *Plant & Cell Physiology* **60**(2), 255–273. doi:10.1093/pcp/pcz001

Handling Editor: Vadim Demidchik